

ICSV14
Cairns • Australia
9-12 July, 2007



USING VIBRATIONAL PROPERTIES OF THE WHEEL TO IDENTIFY TYRE – ROAD FRICTION

Edwin de Vries¹, Daniel Rixen¹, Hiroyuki Katsuno² and Thijs van Keulen^{1,2}

¹Delft University of Technology,
Mekelweg 2, 2628 CD Delft, The Netherlands

²Bridgestone Technical Centre Europe
Via del Fosso Del Salceto 13/15, 00129 Rome, Italy

E.J.H.deVries@tudelft.nl

Abstract

This paper describes the use of vibrations in a single passenger car wheel to identify road friction. The peak in the transfer function of wheel speed to brake torque variations at the lowest resonance frequency (≈ 32 Hz) is strongly influenced by the ‘constraint’ provided by the road surface.

A model of the wheel with its rotational inertia in contact with the road via the tyre is developed. The inflated tyre carcass provides the stiffness in all directions, here mainly the rotational motion of the wheel, combined with the forward motion of the vehicle is considered. The tyre to road interaction includes the effect of saturation in the force versus brake slip characteristic. After linearization it can be proven that the local derivative of the slip characteristic has a consistent influence on the dynamic behaviour of the tyre. Where the local derivative tends to zero, the maximum achievable brake force is reached. Therefore, assessing the local derivative of the brake force versus slip curve is vital for optimal braking.

The phenomenon is also studied in a laboratory environment, with a single braked wheel, running on an electrically driven steel drum of 2.5 m diameter. Special attention is needed for the instrumentation of the wheel rotational speed. To reach the required sample rate and resolution in wheel speed information, the data-acquisition counts the duration of an encoder period. Since this wheel speed signal becomes available at encoder flanges, it needs to be resampled to create data that is synchronous with the input brake pressure and –torque and –force data, typically sampled at 512 Hz.

For some conditions and road surfaces (bare steel and ‘safety walk paper’) both the relation between local derivative and resonance gain and the application of this relation as a friction identification methodology will be assessed.

1. INTRODUCTION

Vehicle braking has been changed by the introduction of driver assistance systems. First anti-lock braking (ABS) was introduced in 1978. Nowadays ABS is incorporated in the electronic stability (ESP) program that now becomes standard component in the mid size passenger cars. The ABS controller will prevent wheel lock as the name suggests; moreover it will try to

control to track the reference slip. The optimal wheel slip will generate the maximum Brake force, but the problem lies in the road surface condition. The road friction will not only influence the force level, but also the slip at which the maximum force will be found. This makes the reference slip dependent on road conditions.

In 1998 Sugai et al. [3] presented an alternative way to control antilock braking. The resonance of the wheel rotation was used as a measure for the adhesion in the road contact. Gustafsson [1] also uses the wheel resonance; he concentrates on the natural frequency of the wheel rotational speed. His wheels are excited by road irregularities only. A relation between natural frequency and tyre inflation pressure was found. Also Unemo et al. [4] presented a pressure diagnosis system based on a Kalman filter.

We want to explain the physical principle of the resonance with a more elaborated model. The consistency of the relation between resonance gain and local slip stiffness is tested in the laboratory on three types of tyres. The information about the slip stiffness tending to zero can be used to define the optimal slip reference value in ABS braking.

2. DYNAMIC MODEL

The resonance frequency considered in this study is the lowest natural frequency of the single tyre-wheel model. In this model the wheel carries a quarter of the vehicle mass and the wheel load transfer that will occur during braking is disregarded. The wheel axle is connected with a revolute joint to the quarter car body. The quarter car body can translate in x and z direction, but restrained from tipping over as it is in real world connected with the rest of the vehicle. On the wheel rim the tyre is mounted. The dynamic tyre model was based on the SWIFT (Short wavelength Intermediate Frequency Tyre) model which was developed in [5]. The objective of the swift model is to describe the transient and dynamic effects in the tyre up to a frequency of 100Hz. At these high frequencies the inertial effects of the tyre cannot be neglected. Therefore the tyre is represented as a suspended rigid ring, see Figure 1. In the paper only the dynamics acting in the wheel plane are modelled. The model consists of two rigid bodies: a ring representing the tyre belt and tread, and an axle body representing the rim, axle and brake disk. The tyre flexible sidewalls represented as springs in vertical longitudinal and torsional direction connect the two bodies. The dynamic tyre model is connected to the contact model via a residual spring.

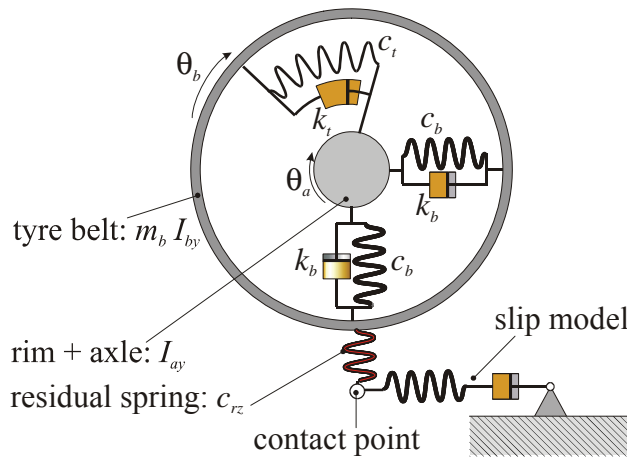


Figure 1 the rigid ring 'SWIFT' model

The equations (1) describe the dynamic tyre model. x and z denote the displacement in horizontal and vertical direction. With a subscript a the variable refers to the axle and with a b to the belt. The angle of rotation θ is introduced, for both axle and tyre belt rotation. The tyre contact forces acting on the belt are denoted by F_{cx} and F_{cz} :

$$\begin{aligned}\ddot{x}_b &= -\frac{1}{m_b} \left(k_b (\dot{x}_b - \dot{x}_a) + c_b (x_b - x_a) - k_z (\dot{\theta}_b) (z_b - z_a) + F_{cx} \right) \\ \ddot{z}_b &= -\frac{1}{m_b} \left(k_b (\dot{z}_b - \dot{z}_a) + c_b (z_b - z_a) + k_z (\dot{\theta}_b) (x_b - x_a) + F_{cz} \right) \\ \ddot{\theta}_b &= -\frac{1}{I_b} k_\theta (\dot{\theta}_b - \dot{\theta}_a) + c_\theta (\theta_b - \theta_a) - r_e F_{cx} - M_{cy} \\ \ddot{\theta}_a &= -\frac{1}{I_a} k_\theta (\dot{\theta}_a - \dot{\theta}_b) + c_\theta (\theta_a - \theta_b) + M_{ay}\end{aligned}\quad (1)$$

With M_{cy} the rolling resistance drag is introduced. To exclude the rigid body motion from the model, the tyre torsional deformation $\theta_a - \theta_b$ results from integrating $\dot{\theta}_a - \dot{\theta}_b$. When we define the wheel as part of a quarter car its equation of motion in horizontal direction is added

$$\ddot{x}_a = -\frac{1}{m_{\frac{1}{4}car}} \left(k_b (\dot{x}_a - \dot{x}_b) + c_b (x_a - x_b) + k_z (\dot{\theta}_b) (z_b - z_a) \right) \quad (2)$$

The description of the stationary behaviour of the tyre is based on the slip ratio, which is the slip speed V_{sx} normalized with the forward speed V_{cx} of the axle:

$$\kappa = \frac{-V_{sx}}{V_{cx}} \quad \text{with } V_{sx} = \dot{x}_b - r_e \dot{\theta}_b \text{ and } V_{cx} = \dot{x}_a \quad (3)$$

The tyre to road contact is here modelled with a relaxation model whose physical effect can be represented as a spring damper in series. The damper produces a force proportional to wheel slip ratio for small slip. Now the transient slip in the contact ζ is defined by applying a first order filter on the stationary slip. The transient slip ζ replaces the stationary slip κ in the force calculation.

$$\dot{\zeta} = \frac{-1}{\sigma_c} (\dot{x}_b - r_e \dot{\theta}_b + |V_{cx}| \zeta) \quad (4)$$

The tyre force is highly nonlinear since the friction coefficient limits the brake force. The tyre force saturation can be described by purely empirical models e.g. Delft tyre model, or a more physics based ‘brush model’. In both descriptions the local derivative of the steady state Brake force versus slip characteristic will decrease for increasing brake force and slip. When the derivative equals zero the maximum brake force will be reached. The Delft tyre model would describe the force decaying for increasing slip beyond the peak slip value. The brush model does not include this negative slope. We will not include the full nonlinear tyre characteristic but we will derive the linear model that would only be valid for small perturbations around the average slip and thus brake torque level.

$$F_{cx} = MF(\zeta) \cong MF(\zeta_m) + \left. \frac{\partial F_x}{\partial \zeta} \right|_{\zeta=\zeta_m} \tilde{\zeta} \quad (5)$$

MF denotes the Delft tyre model, also named *Magic Formula* [2]. $\tilde{\zeta}$ denotes the small variation in slip, and ζ_m defines the operation point. The local slip stiffness is given by $\partial F_x / \partial \zeta$ as a function of average slip level.

The model behaviour is presented in the transfer function of Figure 2. The local slip stiffness is varied from 30.000 to 300.000 N. The driving speed is set at a fixed 30 km/h. At low frequency, in steady-state, the brake force will find equilibrium with the brake torque on the rim. At 32 Hz the first resonance frequency occurs, the mode shape shows mainly the wheel and tyre belt rotating in phase. The strong influence of slip stiffness on the damping of this mode can clearly be seen in the figure.

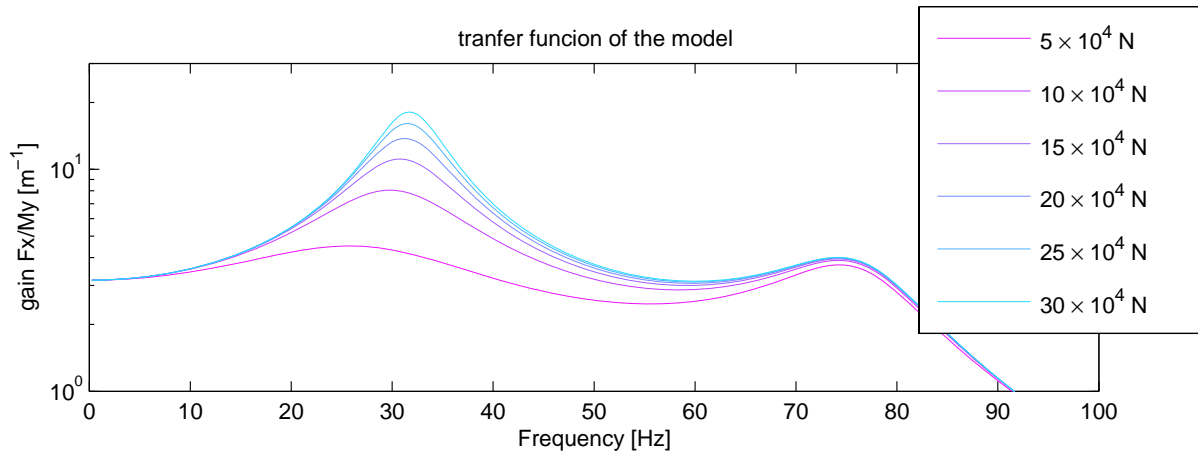


Figure 2 The transfer function of brake force to torque from the model for increasing levels of local slip stiffness given in the legend

3. LABORATORY TESTING

In the Laboratory a test rig is available to measure the tyre dynamic response to brake torque variations. A single wheel runs on a 2.5 m diameter steel drum. The drum speed can be accurately controlled by a large electromotor. The axle position is constraint in all directions. Just the wheel rotation is allowed. This rotation can be braked with a conventional disc brake, the brake fluid pressure being electronically controlled by a small servo-valve.

The sensors available for brake pressure, brake torque, and longitudinal brake force at two sides of the wheel, are indicated in Figure 3 and Figure 4. Having the sensors would allow finding the transfer functions of brake force and wheel speed to brake torque. A future application of the complete method would be restricted to the use of sensors commonly used, or easily (and cheaply) available. Therefore we will concentrate on the wheel speed signal. We will use an industrial optical encoder. The incremental encoder will give 2500 electrical pulses per revolution. With pulse counting the angle and angular velocity can be reconstructed. We can easily show that the considerable number of pulses is barely sufficient to adopt pulse counting with a high sample rate.

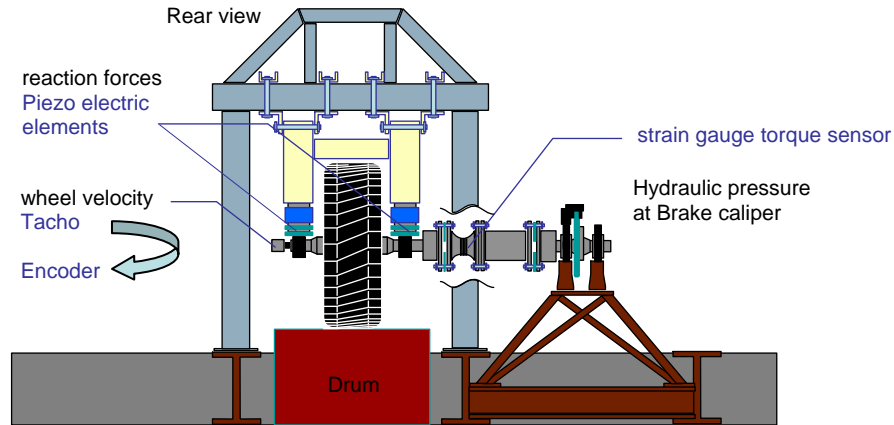


Figure 3 schematic drawing of the single braked wheel test rig in rear view

Suppose a frequency range of interest to 100 Hz; and a sample rate of 250 Hz is used. At 20 m/s the wheel will rotate with 10 revs/sec. Per sample interval 100 pulses can be counted. A speed variation will thus be measured with a discretization error of 1%. Driving slower or sampling at a higher rate will increase the discretization error to unacceptable levels. Therefore we will make use of pulse period width acquisition. The encoder pulse will ‘gate’ the counter of the data acquisition that counts the pulses of its internal clock. This clock frequency is set at 20 MHz. Now the pulse period measured for the case above is $2e7/2.5e4$. The discretization error is here 1.25%, and the accuracy improves when driving slower.

We will excite the system with band pass filtered Gaussian white noise. In Figure 5 a time recording of the wheel rotational speed is presented. One difficulty is the spikes in the measurement. These are caused by ‘mis-triggering’ of the counter. The analogue TTL pulse signal from the encoder is polluted with noise. If a noise peak is large enough it will be misinterpreted as encoder signal flange, the clock counting is stopped and the encoder pulse period is too short. After transformation to rotational speed the calculated speed turns out to be very high to pass $1/n^{th}$ of a revolution in this short time.

The data acquisition will store each encoder pulse period. This implies that the wheel speed data is sampled at fixed angular interval. All analogue data is sampled with 512 Hz. So the wheel speed data needs to be resampled to match this sample rate. The encoder period data will, after it is summed, indicate the time. Based on the reconstructed time we can resample the encoder data. Although the spikes can be detected and replaced by the average of previous and next speed value, the occurrence of mistriggered intervals will disturb the time axis. We think this explains the unacceptable coherence we obtain for the brake torque to wheel speed transfer function.

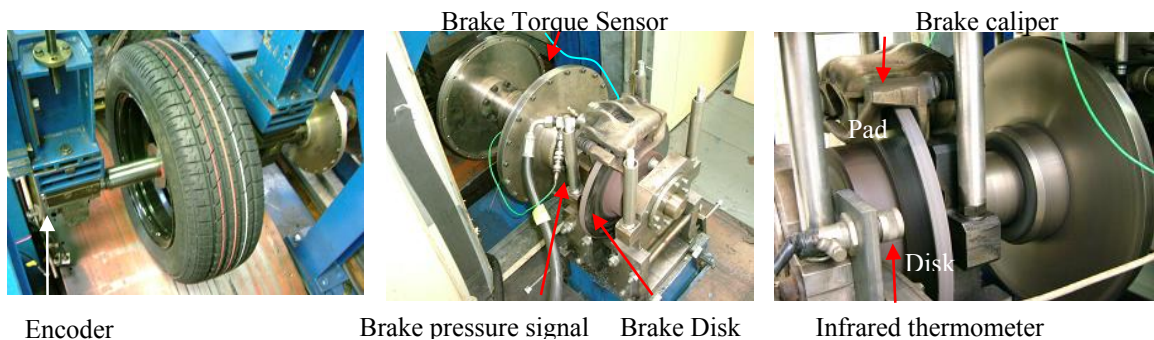


Figure 4 Single braked wheel laboratory test rig

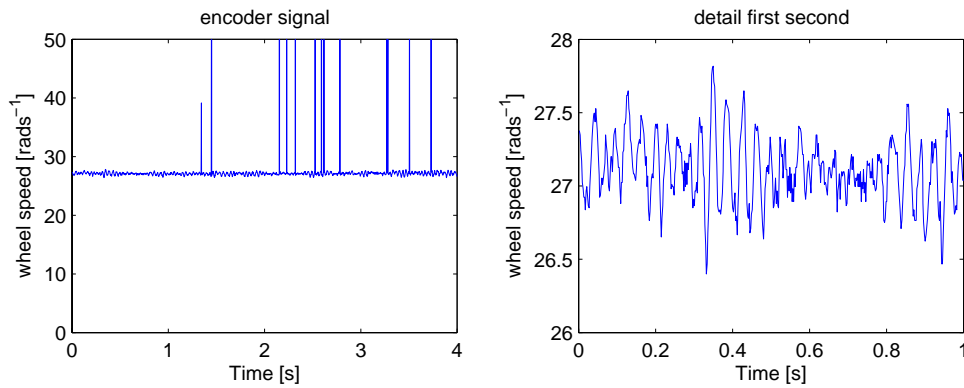


Figure 5 time recording of the wheel rotational speed

Since the wheel speed signal has a too poor correlation with the input, in Figure 6 the brake torque to brake force transfer function has been presented to prove the existence of the resonance and the validity of the model. The FRF is the result from 5 tests of 16 seconds each, sampled at 512 Hz. The test data was windowed with non-overlapping Hanning windows of 2048 datapoints leading to segments of 4 s. each.

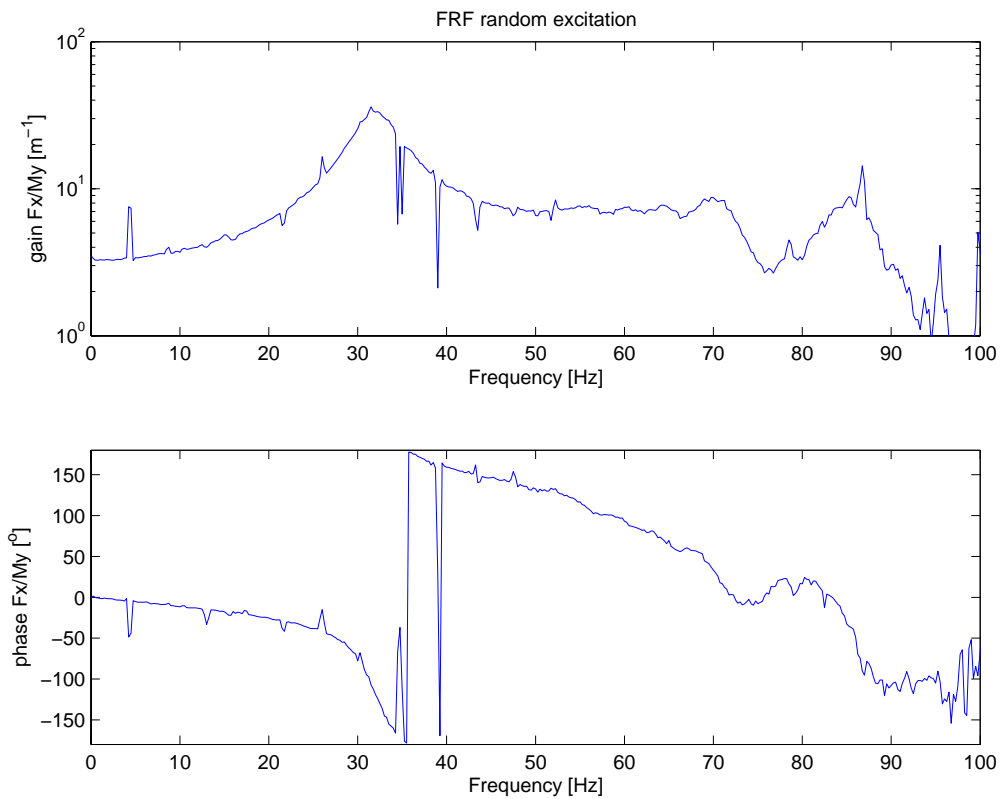


Figure 6 Magnitude and phase of the brake force to -torque FRF with random excitation

At low frequency we can see that a gain of $1/r$ satisfies the stationary equilibrium of the wheel disc. At 32 Hz the resonance frequency occurs. The spikes in this FRF are harmonics of the wheel rotational speed that have their effect due to imbalance or tyre non uniformity forces. The coherence drops considerable at these harmonic frequencies. The coherence of this FRF is above 0.95 for all other frequencies less than 90 Hz. Balancing the wheel could smoothen the transfer function.

For the future application in real time in a vehicle, we will not be allowed to use FFT operations in the software. Therefore we have adopted sinusoidal excitation. The excitation frequency should be chosen to match the resonance frequency beforehand. The gain can be derived by sine-cosine correlation or by peak-peak detection. The first method would suppress noise with other than the excitation frequency; depending also on the time interval used. However the latter method is used here to obtain the transfer data.

In Figure 7 the final result of sinusoidal testing is given. At each operating condition, represented as an average brake pressure level, the brake pressure has been perturbed by a sinusoidal variation of 10 bar (resulting in 50 Nm) with a frequency of 20 25 28 30 32 and 40 Hz respectively. We can now clearly observe the decreasing resonance at higher average brake pressure levels. The same property as we have presented with the model is now shown in laboratory practice. For this method to be predictive we need to define the relation between resonance gain and local slip stiffness. If the local slip stiffness tends to zero we reach the maximum of brake force.

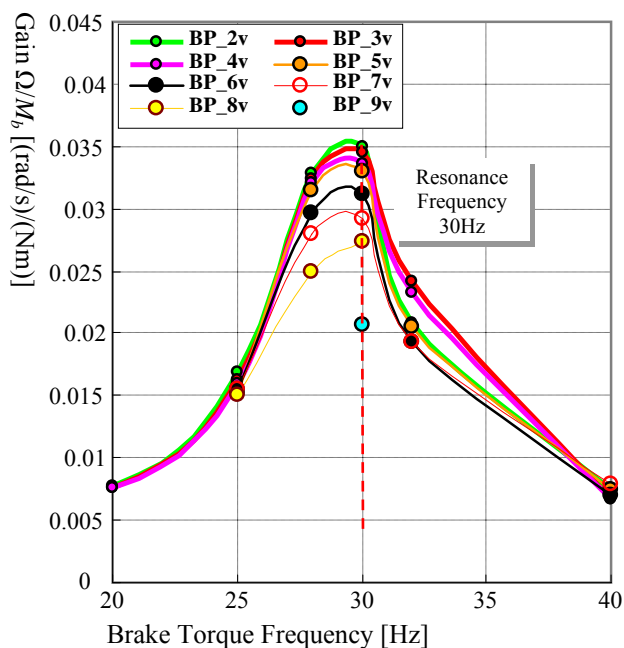


Figure 7 The gain of wheel rotational speed (Ω) to brake torque during sinusoidal excitation

The relation between local slip stiffness and resonance gain is presented in Figure 8b for three different passenger car tyres of size 195/65 R 15. In the operation condition we can measure average brake force and wheel speed. One extra experiment at free rolling ($\kappa = 0$) is necessary to find the value of r_e empirically; using equation 3 at $\kappa = 0$. With the value of r_e fixed the slip κ can be calculated in all experiments. In Figure 8a the average brake force has been plotted against slip to obtain the brake slip characteristic. Now a quadratic approximation is made and the analytical derivative is calculated at the slip levels in the operating points. This value will serve as local slip stiffness in the experiment and is used on the horizontal axis of figure 8b.

All tyres that were tested on a safety walk paper drum surface show a quite consistent relation. In using the proposed identification to define optimal reference slip or brake pressure a lower threshold should be defined. Therefore we would not look for the intersection at the origin but maybe at a gain smaller than 0.005. Here the three tyre behave quite consistent on safety walk paper. One tyre has been tested on a bare steel drum surface, results indicated with the open bullets in Figure 8. Although we did not reach average brake force levels high enough, it seems that this drum surface produces a relation that differs from the three others.

We should thus further investigate the effect of road surface properties on the relation between resonance gain and slip stiffness.

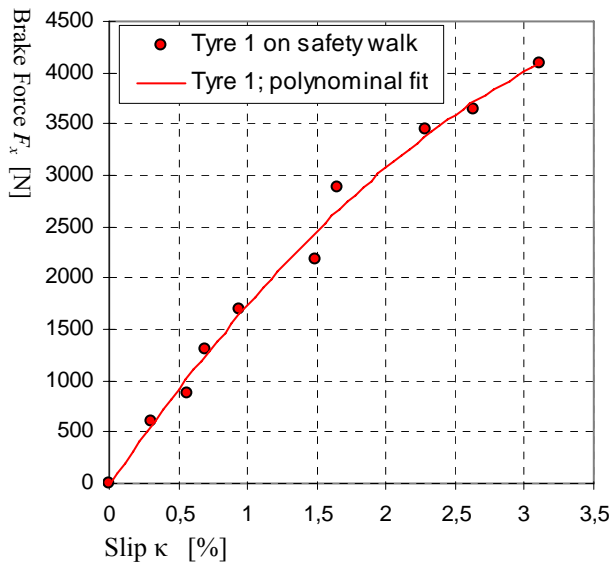


Figure 8a The brake force characteristic

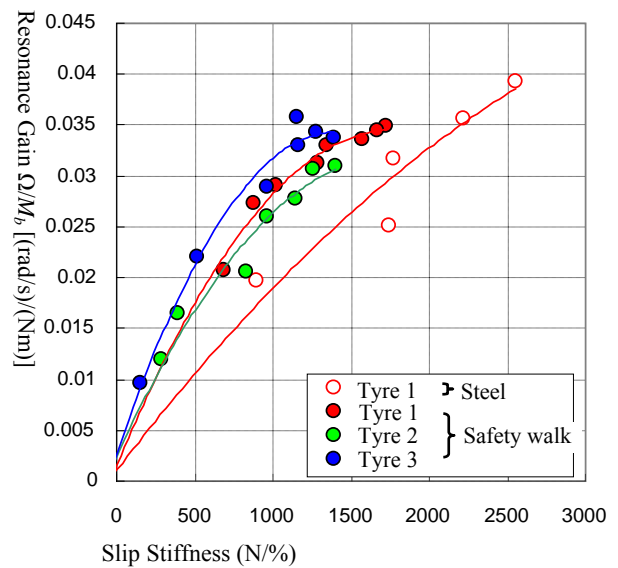


Figure 8b The relation found between resonance gain and local slip stiffness

CONCLUSIONS AND RECOMMENDATIONS

The single braked wheel showing a lower resonance gain at decreasing slip stiffness has been presented as a property brake wheel model. This property has been validated in laboratory testing. For model validation random excitation was used, an accurate transfer function of wheel rotational speed could not be obtained. The reconstruction of the time axis from the encoder period signal will suffer from a varying bias due to missing or mis-triggered periods. Therefore the correlation between input and output is lost. To prove the existence of the resonance and the validity of the model the transfer function from brake torque to brake force has been presented.

For the application in a vehicle the real time data processing (FFT) of a random signal would demand too much calculation effort. With sinusoidal excitation a very simple calculation is used to find the gain. The disadvantage is that the excitation frequency has to be chosen right at the resonance beforehand. Three tyres show a consistent relation between gain and local slip stiffness in Laboratory testing on safety walk paper. Some tests on bare steel drum surface deviate somewhat. The resonance properties on a bare steel drum and on other road surfaces should be investigated more closely.

For a further application as friction observer we have to relate the operating point at which we see the slip stiffness tending to zero with the friction coefficient. We need in the operating point the longitudinal and vertical force, their ratio is defined as friction coefficient. Only our laboratory test these forces are measured. In a car these forces need to be identified. With this information the normalized brake force characteristic can be identified, but the added value of the resonance identification is that the actual maximum of the force can be marked when it occurs, without having to pass it and running into suboptimal operation points.

The resonance relates to the slip stiffness consistently and can therefore be used successfully to indicate the maximum achievable brake force.

REFERENCES

- [1] F. Gustafsson, M. Drevo, U. Forssell, M. Löfgren, N. Persson, H. Quicklund, “Virtual sensors of tire pressure and road friction” *SAE paper* 2001-01-0796.
- [2] H.B. Pacejka, E. Bakker, “The magic formula tyre model”, *Proceedings 1st Tyre colloquium*, Delft, The Netherlands, Oct 1991 suppl. to *Vehicle System Dynamics* vol. 21, 1993
- [3] M. Sugai, H. Yamaguchi, M. Miyashita, T. Unemo and K. Asano, “New Control Technique for Maximizing Braking Force on Antilock Braking system”, *Proceedings AVEC 1998*, Nagoya, Japan, 14–18 September 1998, pp. 649-654.
- [4] T. Unemo, K. Asano, H. Ohashi, M. Yonetani, T. Naitou, T. Taguchi “Observer based estimation of parameter variations and its application to tyre pressure diagnosis”, *Control Engineering Practice* 9, 639-645 (2001).
- [5] P.W.A. Zegelaar, *The dynamic response of tyres to brake torque variations and road unevennesses*, PhD thesis, Delft University of Technology, Delft, 1998.